SEM Study of a Polystyrene/Clay Nanocomposite

JIAQI FAN, SUHUAI LIU, GUANGMING CHEN, ZONGNENG QI

State Key Laboratory of Engineering Plastics, Center for Molecular Science, Chinese Academy of Sciences, Beijing 100080, People's Republic of China

Received 17 January 2000; accepted 16 March 2001

ABSTRACT: We carried out a scanning electron microscopy study to investigate the morphology of a polystyrene (PS)/montmorillonite nanocomposite. Monodispersed spherical particles, about 200 nm in diameter, were observed when PS/montmorillonite powder was dispersed in water, whereas planar silicate sheets were found for cetyltrimethylammonium bromide-exchange montmorillonite. The fracture surface of a PS/clay nanocomposite pellet sample showed a lot of fibrils rather than the smooth surface of a pure PS pellet. After the PS/clay nanocomposite pellet was chemically etched, flaky montmorillonite particles were homogeneously dispersed in the PS matrix. A film sample, prepared by the pressing of the PS/clay nanocomposite melt, revealed that the montmorillonite primary particles oriented parallel to the surface, and the corresponding X-ray diffraction distribution map of silicon atoms confirmed that the dispersed particles were montmorillonite primary particles. © 2002 John Wiley & Sons, Inc. J Appl Polym Sci 83: 66–69, 2002

Key words: polystyrene; clay; nanocomposites; scanning electron microscopy (SEM)

INTRODUCTION

Polymer/clay nanocomposites have recently attracted much interest over a wide range of scientific and practical viewpoints, such as structured[1–4] and conductive materials,[5] since the development of a nylon-6/clay nanocomposite by Toyota researchers.[1–4] They exhibit dramatically increasing mechanical, thermal, and gas/liquid barrier properties[6–9] and unusual chemical and physical phenomena[10,11] that typically are not shared by their conventional macrocomposite and microcomposite counterparts. Thus, they may bring new opportunities in high technology and business applications. For example, Toyota Motor Co. has applied a nylon/clay nanocomposite to an automotive timing-belt cover.[12]

Montmorillonite is a commonly used clay. Its layer structure is constructed of an octahedral alumina sheet sandwiched between two tetrahedral silica sheets. Stacking of layers about 1 nm thick by a weak dipolar force leads to interlayer galleries.[13] The galleries are normally occupied by such cations as Na^+, Ca^{2+}, and Mg^{2+}. Organomontmorillonite is obtained with a cation-exchange reaction or the adsorption of small alkylammonium or other organic cations into the interlamellar spacings.[14,15] During *in situ* intercalative polymerization or melt intercalation, montmorillonite can be broken down into nanoscale building blocks and dispersed homogeneously in a polymer matrix to afford polymer/clay nanocomposites. The unusual mechanical properties are generally attributed to

Throughout this article, we use the term *primary particles* to describe the microstructure features of the silicate crystallites. The crystallites consist of a coherent stacking of individual silicate layers, including compact face-to-face stacking and low-angle intergrowth of silicate layers.

Correspondence to: Z. Qi.

Contract grant sponsor: National Natural Science Foundation of China; contract grant number: 59833130.

Journal of Applied Polymer Science, Vol. 83, 66–69 (2002)

the homogeneous dispersion of the silicate nanoscale particles.[16]

We recently prepared a polystyrene (PS)/montmorillonite nanocomposite via an *in situ* intercalative polymerization method,[17] and the product was characterized by X-ray diffraction and transmission electron microscopy techniques. Additionally, a unique shear-induced ordered structure[18–21] and a self-assembly behavior with increasing temperature[22] were unexpectedly observed for the pellet sample.

Scanning electron microscopy (SEM) has many advantages in morphology investigations.[23] Compared with optical microscopy and transmission electron microscopy, it has such advantages as great depth of focus and ease of specimen preparation. Therefore, it has been extensively applied in the fields of metallurgy, fibers and polymers, solid-state electronics, biological materials, composites, and so forth.[23] In this article, we report a SEM study of a PS/clay nanocomposite. First, a SEM micrograph of the powder sample is presented, and then the fracture surfaces are studied of the pellet and film samples both before and after chemical etching, combined with X-ray mapping of the distribution of the silicon.

EXPERIMENTAL

Materials and Samples

Sodium montmorillonite (Swy-2 type) was kindly provided by the Source Clay Repository of the Department of Geology at the University of Missouri (Columbia, MO). Its cation-exchange capacity (CEC) was 92 mequiv/100 g. Styrene monomer was purified by distillation under reduced pressure in a nitrogen atmosphere before use. All of the chemicals used in this investigation were analytical-reagent-grade.

The ion exchange of Na^+ of montmorillonite with cetyltrimethylammonium bromide (CTAB), the synthesis procedure of the PS/montmorillonite nanocomposite via the *in situ* intercalative polymerization method, and the preparation of the pellet specimens are described in our previous studies.[17–22] CTAB–montmorillonite was prepared by the conventional ion-exchange method; that is, after an amount of CTAB equivalent to the CEC of the Na–montmorillonite suspension was added and after stirring for 1 day, the suspension was filtered, washed three times with distilled water, dried in a vacuum oven, and ground. The PS/montmorillonite nanocomposite containing 5 wt % CTAB–montmorillonite was prepared by the *in situ* intercalative polymerization process. CTAB–montmorillonite was dispersed in styrene monomer and dispersed fully into a stable transparent dispersion; this allowed the styrene monomer to intercalate into the CTAB–montmorillonite galleries. Then, an aqueous mixture of ammonium persulfate $[(NH_4)_2S_2O_8]$ as a radical initiator and sodium dodecyl sulfate as an emulsifying agent were added; the resulting mixture was stirred vigorously at room temperature for 30 min and subsequently polymerized at 70–80°C for 5 h under a N_2 atmosphere. Finally, the product was obtained after being washed, dried, and crushed. The pellet specimens of the PS/montmorillonite nanocomposites were prepared by extrusion of the PS/montmorillonite nanocomposite powder at 200°C with a CS-183 MMX Mini Max Molder (CSI Custom Scientific Instruments, Inc., United States). They were about 1.5 mm thick, 20–25 mm long, and 12 mm wide. The film specimens were prepared by the PS/clay nanocomposite melt being pressed between two glass slides at about 200°C and subsequently being quickly cooled down in cold water and chemically etched in toluene.

SEM Investigations

The morphology of the PS/clay nanocomposite was examined with a JEOL 0301 scanning electron microscope (JEOL USA, Inc., Peabody, MA) equipped with an energy-dispersive X-ray detector. The acceleration voltage was 20 kV. A secondary electron emission was collected, and the resolution of the image was 1.5 nm.

The synthesized powder sample was fully dispersed in distilled water, ultrasonically homogenized, and deposited on an aluminum film. The pellet samples were fractured after immersion in liquid nitrogen. Then, parts of the samples were coated with gold, and other parts of the samples

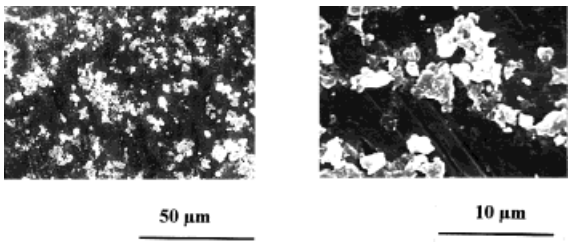

Figure 1 SEM micrographs of CTAB-exchanged montmorillonite powder.

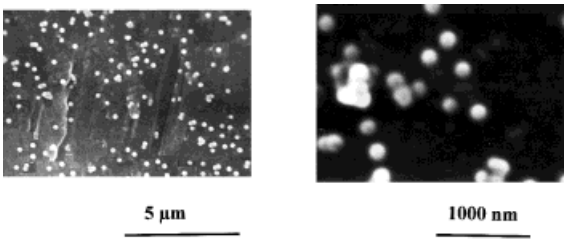

Figure 2 SEM micrographs of the PS/montmorillonite nanocomposite powder sample.

were coated with gold after being etched with toluene to expose possibly concealed montmorillonite nanosized particles.

RESULTS AND DISCUSSION

Figure 1 shows the morphology of the dispersed CTAB–montmorillonite powder in an aqueous suspension. The planar montmorillonite aggregates are prevalent. The montmorillonite aggregates have high aspect ratios. Unlike rigid plates, most of the aggregates are dark in the center and light in the boundary, showing some flexibility. Figure 2 presents the SEM micrographs of the PS/montmorillonite nanocomposite powder sample. The synthesized product via emulsion polymerization is monodispersed spherical particles. These spherical particles are about 200 nm in diameter.

The fracture surface of the extruded pure PS pellet is shown in Figure 3. The fracture surface is relatively even and smooth, showing a typical brittle fracture feature. Figure 4 presents SEM microphotographs of the PS/montmorillonite nanocomposite pellet sample before it was chemically etched. Fibrils leading to stress whitening are prevalent in Figure 4, indicating localized plastic deformation. This indicates that the nanocomposite may have some degree of toughness in comparison with pure PS.

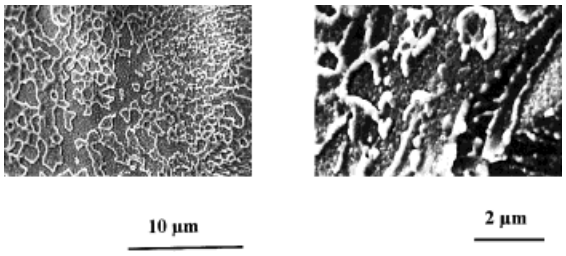

Figure 3 SEM photographs of the fracture surface of pure PS.

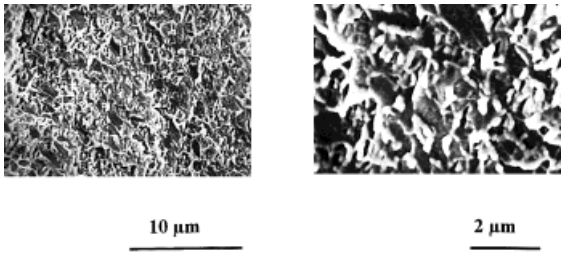

Figure 4 SEM photographs of the fracture surface of the PS/montmorillonite nanocomposite pellet sample before it was chemically etched.

After the fractured pellet sample of the PS/clay nanocomposite was chemically etched by toluene, the fibrils dissolved, and the montmorillonite primary particles can be clearly observed, as shown in Figure 5. During the intercalative polymerization process, the layer structure of the montmorillonite suffered tremendous damage and was exfoliated from expansion induced by the PS molecular size increasing and the exothermal reaction between the galleries.[17–19] Figure 5 shows that after polymerization, the micron montmorillonite aggregates are broken into small particles and dispersed homogeneously in the PS matrix. This is in agreement with our previous transmission electron microscopy studies.[18,19] To observe more details of these silicate primary particles, we present Figure 5(b) with a higher magnification. The length of the primary particles is less than 350 nm. Because the planar silicate primary particles disperse in every direction and appear to be flexible, it is difficult to determine the thickness directly from SEM micrographs.

Figure 6 presents the surface morphology of the PS/montmorillonite nanocomposite film specimen. Because the specimen was prepared via

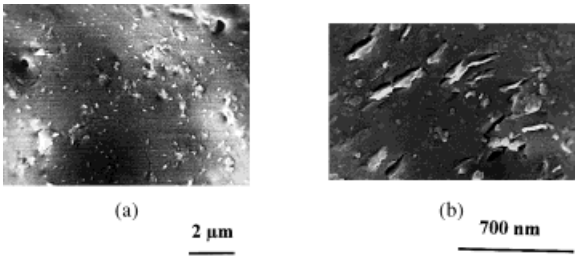

Figure 5 SEM photographs of the fracture surface of the PS/montmorillonite nanocomposite pellet sample after it was chemically etched.

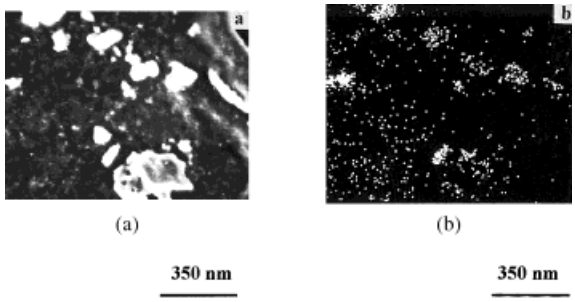

Figure 6 (a) SEM micrograph of the etched PS/montmorillonite nanocomposite film sample and (b) its X-ray mapping, which shows the distribution of the silicon.

pressing of the melt, the montmorillonite primary particles prefer an orientation parallel to the film surface. It can be seen from Figure 6(a) that the diameter of the planar montmorillonite primary particles is less than 350 nm. This is quite consistent with the above-mentioned results of Figure 5. The distribution of the montmorillonite primary particles in Figure 6(a) was aided by an energy-dispersive X-ray probe. An image of elemental mapping for Si is shown in Figure 6(b). The domains of the little white dots in Figure 6(b), representative of Si, correspond to the dispersed phase in Figure 6(a) very well. This indicates that the domains are the images of the montmorillonite primary particles.

CONCLUSIONS

The synthesized PS/montmorillonite powder was composed of monodispersed spherical particles about 200 nm in diameter. Before the PS/montmorillonite nanocomposite pellet was chemically etched, the fracture surface showed many fibrils in comparison with the smooth surface of pure PS. After the PS/montmorillonite pellet fractured surface was chemically etched, the homogeneously dispersed montmorillonite primary particles could be clearly observed. As for the etched film sample, the primary particles preferred an orientation parallel to the surface.

REFERENCES

1. Okada, A.; Kawasumi, M.; Kurauchi, T.; Kamingaito, O. Polym Prepr 1987, 28, 447.
2. Usuki, A.; Kawasumi, M.; Kojima, Y.; Okada, A.; Kurauchi, T.; Kamingaito, O. J Mater Res 1993, 8, 1174.
3. Usuki, A.; Kojima, Y.; Kawasumi, M.; Okada, A.; Fukushima, Y.; Kurauchi, T.; Kamingaito, O. J Mater Res 1993, 8, 1179.
4. Kojima, Y.; Usuki, A.; Kawasumi, M.; Okada, A.; Fukushima, Y.; Kurauchi, T.; Kamingaito O. J Mater Res 1993, 8, 1185.
5. Ruiz-Hitzky, E.; Aranda, P.; Casal, B.; Galvan, C. Adv Mater 1995, 7, 180.
6. Giannelis, E. P. Adv Mater 1996, 8, 29.
7. Chen, G.; Li, Q.; Qi, Z.; Wang, F. Polym Bull 1999, 4, 1 (in Chinese with an English abstract).
8. Lan, T.; Kaviratna, P. D.; Pinnavaia, T. J. Chem Mater 1994, 6, 573.
9. Chen, G.; Ma, Y.; Liu, S.; Qi, Z. J Appl Polym Sci 2000, 77, 2201.
10. Mehrotra, V.; Giannelis, E. P. Solid State Commun 1991, 77, 155.
11. Miyata, H.; Sugahara, Y.; Kuroda, K.; Kato, C. J Chem Soc Faraday Trans 1987, 83, 1851.
12. Kurauchi, T.; Okada, A.; Nomura, T.; Nishio, T.; Saegusa, S.; Deguchi, R. Soc Automot Eng Tech Pap Ser 1991, 910584.
13. Grim, R. E. Clay Mineralogy; McGraw-Hill: New York, 1968.
14. Chen, G.; Han, B.; Yan, H. J Colloid Interface Sci 1998, 201, 158.
15. Chen, G.; Song X.; Zhao, Y.; Han, B.; Yan, H. J Colloid Interface Sci 1997, 186, 206.
16. Dagani, R. Chem Eng News 1999, 77(23), 25.
17. Qi, Z.; Wang, F.; Ma, Y.; Chen, G. Chin. Pat. 98103038.6 (1998).
18. Chen, G.; Shen, D.; Qi, Z. J Mater Res 2000, 2, 351.
19. Chen, G.; Qi, Z. Chem J Chin Univ 1999, 20, 1987 (in Chinese with an English abstract).
20. Chen, G.; Shen, D.; Chen, S.; Qi, Z. Chem J Chin Univ 2000, 4, 657 (in Chinese with an English abstract).
21. Chen, G.; Ma, Y.; Qi, Z. Proc. Fifth IUMRS International Conference on Advanced Materials, Beijing, 1999, p 572.
22. Chen, G.; Liu, S.; Zhang, S.; Qi, Z. Macromolecular Rapid Commun 2000, 21, 746.
23. Hearle, J. W. S.; Sparrow, J. T.; Cross, P. M. The Use of the Scanning Electron Microscope; Pergamon: Oxford, 1972.